Design, development, and testing of the DCT Cassegrain instrument support assembly

Thomas A. Bida, Edward W. Dunham, Ralph A. Nye, Tomas Chylek, and Richard C. Oliver
Lowell Observatory, 1400 West Mars Hill Road, Flagstaff, AZ 86001, USA

ABSTRACT

The 4.3m Discovery Channel Telescope delivers an f/6.1 unvignetted 0.5° field to its RC focal plane. In order to support guiding, wavefront sensing, and instrument installations, a Cassegrain instrument support assembly has been developed which includes a facility guider and wavefront sensor package (GWAVES) and multiple interfaces for instrumentation. A 2-element, all-spherical, fused-silica corrector compensates for field curvature and astigmatism over the 0.5° FOV, while reducing ghost pupil reflections to minimal levels. Dual roving GWAVES camera probes pick off stars in the outer annulus of the corrected field, providing simultaneous guiding and wavefront sensing for telescope operations. The instrument cube supports 5 co-mounted instruments with rapid feed selection via deployable fold mirrors.   The corrected beam passes through a dual filter wheel before imaging with the 6K x 6K single CCD of the Large Monolithic Imager (LMI). We describe key development strategies for the DCT Cassegrain instrument assembly and GWAVES, including construction of a prime focus test assembly with wavefront sensor utilized in fall 2011 to begin characterization of the DCT primary mirror support. We also report on 2012 on-sky test results of wavefront sensing, guiding, and imaging with the integrated Cassegrain cube.

Keywords: DCT, Discovery Channel Telescope, Lowell Observatory, Optical design, Guider, Wavefront sensor, Corrector, Instrument support

1. INTRODUCTION

The 4.3m Discovery Channel Telescope (DCT), an f/6.1 Ritchey-Chretien (RC) design, is fully assembled and operational with coated primary and secondary mirrors, and undergoing its test phase at the Happy Jack site in Northern Arizona (elevation 2361m)[1,2].   The telescope is ultimately capable of supporting instrumentation at the Cassegrain, Prime Focus, and Nasmyth foci. The initial suite of instruments will be implemented at the Cassegrain focus, supported by an instrument interface assembly that can hold 5 co-mounted instruments, and which provides integrated RC correcting optics for one wide-field (up to a 0.5° diameter) instrument, and relay and/or dichroic optics for 4 smaller-field (3 arcmin diameter) instruments. The RC instrument support assembly incorporates the DCT facility guider and wavefront sensor instrumentation (GWAVES), which will be heavily utilized during commissioning to characterize the telescope optical performance, and during regular science operations for mount guiding and real-time wavefront sensing corrections to the optics. This paper will describe the design process for GWAVES (Section 2), the instrument cube assembly (Section 3), the RC corrector optics (Section 4), the CCD camera probes (Section 5), and dedicated DCT test instrumentation and on-sky results obtained throughout the test period at prime focus and with the integrated Cassegrain cube on the completed DCT (Section 6).

2. THE DCT FACILITY GUIDER AND WAVEFRONT SENSORS

The DCT RC guider and wavefront sensing system (GWAVES) is composed of two identical custom camera assemblies mounted on 3-axis positioning and focus stages, and integrated with the instrument mounting cube at the RC focus of the telescope. The system has the capability of simultaneously acquiring and analyzing guide and wavefront sensing stars during operation of instruments mounted on all ports on the cube. The field of acquisition of the GWAVES probes are within the field-of-view (FOV) of the RC corrector that feeds the straight through instrument cube position. Each probe can function as either a guider or wavefront sensor, and the camera and motor components are software-controlled from

Lowell-developed instrument control systems. Derived parameters such as guide star position, and polynomials describing the M1 surface and M2 alignment, will be output to the telescope control system (TCS) for feedback into the telescope tracking drives and M1/M2 active optical system (AOS). Guided telescope offsets and non-sidereal guiding are two of the additional functions supported by the system.

The development of GWAVES was intimately associated with the optical and mechanical design of the RC instrument configuration, including integration with the Large Monolithic Imager (LMI), a 6K x 6K CCD camera with an integral RC field corrector for the DCT[3]. In addition, the system must serve a suite of additional instruments mounted on 4 folded-beam ports located ahead of the RC corrector. The GWAVES system also must meet requirements that were directly driven by DCT performance specifications. The GWAVES system requirements were compiled from a combination of the above considerations[4], leading to the mechanical, electrical, and software specifications for the system. Some specifications were mixed early on with requirements since the LMI design necessarily included GWAVES. A subset of the GWAVES requirements are shown in Table 1, including the driving and as-built specifications.

Table 1. DCT Performance Specifications, and GWAVES Requirements and Operating Specifications		
DCT Performance Specification	GWAVES Requirement	GWAVES Current Specification
Slew velocity: 1.5 deg s[-1] Settle time: 5 s	Probe reposition in < 10 s	X/Y stage velocity: 10 mm/s (15 s 1/2-FOV motion). AOS M1P settling time: up to 17s
Pointing blind accuracy: < 2 arcsec	Probe blind accuracy: < 2 arcsec (250 μm)	Fine-pitch lead-screw driven stages with linear encoders meet requirement
Offset accuracy: < 0.2 arcsec (1 deg) < 0.1 arcsec (0.5 deg)	Probe offset accuracy: < 0.1 arcsec (12 μm)	Stage accuracy: 6 μm
Az/El encoder resolutions: < 0.02 arcsec RMS	Guiding precision: 0.01 arcsec RMS	Camera sensitivity fully modeled (see text) and meets requirement
Guided trajectory update: 1 Hz	Guiding update rate: 1 Hz	Simple guiding tested at 1 Hz
Closed loop image smear: < 0.052 arcsec RMS	Guiding precision: < 0.01 arcsec RMS	Camera sensitivity fully modeled (see text)
AOS update cadence: 30 s	WFS cadence: 30 s	WFS testing cadence: 20 s Operational cadence: 30 s
AOS wavefront precision: < 0.01 arcsec FWHM	WFS centroid precision: < 0.02 arcsec FWHM	WFS sensitivity fully modeled (see text)

The sensitivity of the GWAVES cameras and the FOV available to the moving probes were fully modeled in order to estimate the availability of guide and wavefront sensing stars during operations. The sensitivity of the camera determines the limiting magnitude of guide and WFS stars for a given frame rate and centroid precision. The signal-to-noise ratio (SNR) model for the cameras included a conservative estimate of optical throughput including 60% scattering losses, full-moon sky brightness, and estimated CCD operating parameters (Table 2). The peak pixel SNR required to measure the centroid of an imaged point spread function is[4]: SNR pixel^{-1} = 1.2 * (RMS centroid error (pixels))$^{-1}$.

Table 2. Signal-to-noise ratio calculation parameters	
V-band filter central wavelength	5370 A
V-band transmission width	940 A
Total optical throughput	0.13
Sky brightness, 14d (full moon)	20 mag/arcsec2
Image FWHM	0.84, 1.5 arcsec
CCD format	e2v CCD67, 256^2 26μm pixels
Plate scale	0.336 arcsec/pixel
Dark current	8 e-/s/pixel
Read noise	10 e-

For a 26μm pixel size and guider plate scale of 0.077mm/arcsec, a guiding precision of 0.01 arcsec RMS yields a centroid error of 0.03 pixel at SNR=40 pixel^{-1}. This peak pixel SNR is achieved at a limiting V-magnitude (M_V) of 15.0

for site median seeing of 0.84 arcsec, and 13.7 for 1.5 arcsec seeing. The FOV available to the guide probes for LMI operation is shown in Figure 1, totaling 0.153 deg^2. Utilizing the UCAC3 catalog, 137 stars with $M_V < 15$ are found within 1 deg^2 for the galactic pole, indicating that 21 guide stars should be available in a low stellar density region of the sky. For folded port operation, the available guide star sky area is reduced to 0.12 deg^2, leading to an estimate of 8 guide stars accessible per probe in sparsely populated regions with median seeing.
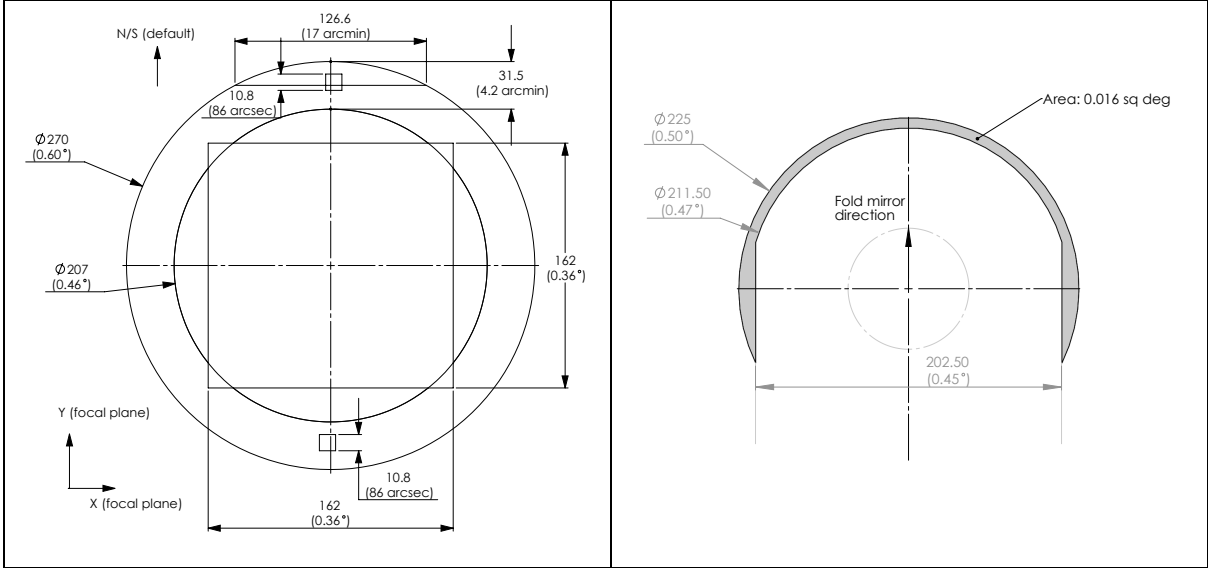
Figure 1. Diagrams of the FOV available to the GWAVES probes, located in between the RC corrector and the Large Monolithic Imager (LMI) camera. Left: the FOV availabe for guide star acquisition during operation of the LMI, totaling 0.153 deg^2; the inner 0.36 deg square represents the unvignetted field of the LMI. Right: the unvignetted FOV available for WFS acquisition during operation of instruments at the folded port locations, totaling 0.016 deg^2.
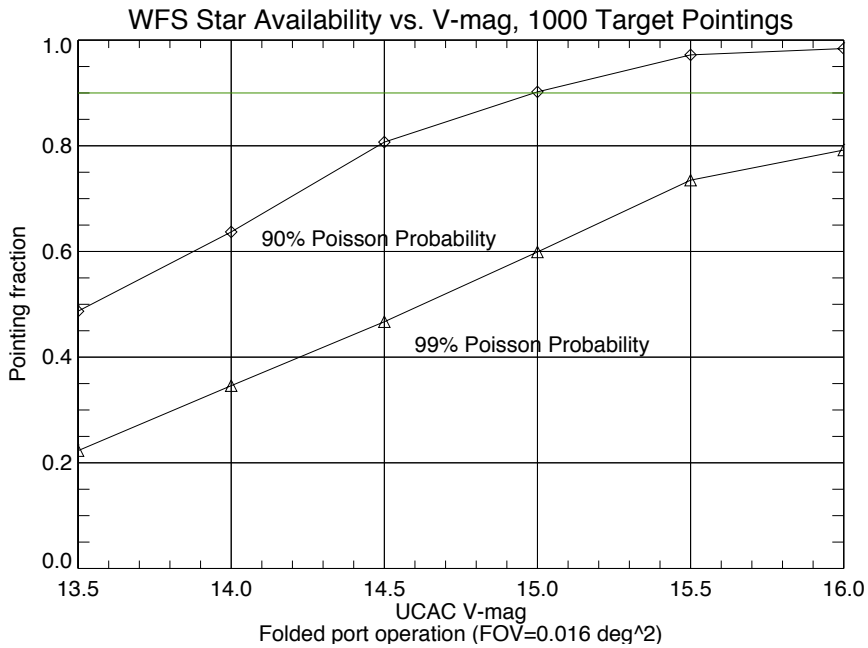
Figure 2. The probability of finding a wavefront sensing star of a given magnitude based on the available unvignetted field of view of the GWAVES probe during folded port operations. The graph indicates that a 90% probability of finding a wavefront star over 90% of the sky occurs at a V-magnitude of 15.

For wavefront sensing, the DCT AOS will be updated at 30s intervals, but the necessary unvignetted FOV available to the GWAVES probes is substantially reduced, to 0.016 deg^2 for folded port operations (Figure 1). The wavefront sensor will operate unfiltered, with a field stop of 8 arcsec diameter at focus to reduce the sky background in each lenslet image which is proportional to the total sky area entering the MLM array. We calculated the fraction of 1000 target pointings generated with a Monte Carlo model to Dec=-50° in the GWAVES star catalog that have a WFS star in the 0.016 deg^2 FOV with 90% and 99% Poisson probabilities over some magnitude range, shown in Figure 2. At 90% Poisson probability, 90% of pointings have stars to $M_V < 15$, and 97% at $M_V < 15.5$. The WFS star limiting magnitudes generated from a broadband SNR model vs. WFS precision and exposure time are shown in Figure 3. At 30s exposure times, 90% target fraction at an acquisition probability of 90% can be achieved at 0.02 arcsec FWHM precision ($M_V < 15$ limit). Although this relaxes the AOS requirement for wavefront sensing precision, in practice the measured wavefront expansion will realistically achieve RMS solutions no better than 0.02 arcsec FWHM.
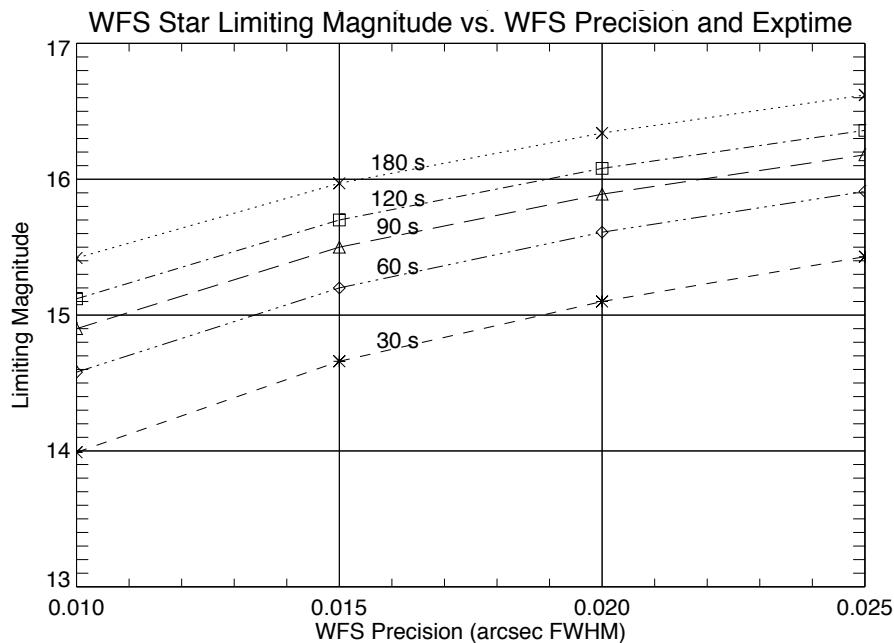

Figure 3. Limiting magnitude vs. wavefront sensing precision, based on centroiding precision of the Shack-Hartmann spots. The required update cycle for DCT wavefront sensing is 2 times/minute (30s integrations), at 0.02 arcsec precision, with a corresponding limiting magnitude of 15.1.

3. DCT RC Instrument Cube

The first-light RC configuration for the DCT, with instrumentation installed at the Cassegrain focus, required development of the RC instrument support assembly, more commonly referred to as the instrument cube. The instrument cube must provide the mechanical, optical, and electronic interfaces for a variety of instrumentation, including two GWAVES probe assemblies. Up to five "hot" operational instruments will be co-mounted on the cube, each instrument rapidly selectable with remote control of custom fold mirrors. This design provides a nearly-unique DCT capability of multi-instrument studies of objects in the same night, including simultaneous optical imaging with the LMI by use of a dichroic in place of the fold mirror.

The optical-mechanical layout of the instrument cube was determined by interdependence of the focal plane locations of the LMI, the guider and wavefront sensors, and the folded instrument ports.   First, the back focal distance from the

Cassegrain rotator flange is 900mm, defining the approximate location of the LMI CCD. The RC corrector optics must be large enough to cover the full unvignetted 0.5° DCT FOV, to provide good optical quality for stars located outside the FOV of the LMI camera for analysis by the GWAVES guider and wavefront sensor probes. The GWAVES probe pickoff mirrors are located behind the RC corrector, and in front of the LMI shutter and dual filter wheel, and rove on an intermediate plane by means of motorized translation stages.   The folded instrument ports must be located forward of the RC corrector, with space to install fold mirror stages and provide sufficient back focus from the instrument mounting surfaces. The instrument cube must be a light, stiff structure, capable of supporting the GWAVES assemblies, the RC corrector and cells, 4 fold mirror assemblies, the LMI dual filter wheel and dewar, and 600kg of additional astronomical instrumentation. The total mass allocation for the Cassegrain instrument assembly is 1500kg, and the instrument envelope is approximately a cylinder 3000mm wide and 1050mm deep, with a 300mm-deep hemispherical cap below.

The as-built instrument cube assembly model, with the LMI installed at the straight through focal position, is shown in Figure 4. The cube is a bolted Aluminum 6061-T6 structure with a 1.5" thick flange, 0.75" wall and support thicknesses, 8 large support gussets, 2 internal 0.75" bulkheads, and constructed with close-fit (0.010") groove joints for tightness and scattered light rejection. The straight through focus is designed to support the LMI dual filter wheel and CCD camera dewar assembly, although other instruments can also utilize that port. In fact, the first-light observations undertaken in April 2012 were accomplished with Lowell's NASA42 instrument, a 4K x 4K CCD camera in regular operation at the Hall 42" telescope, installed behind the LMI dual filter wheel. The LMI filter wheel assembly is 60mm thick, and can hold 20 121mm square filters up to 10mm thick each.
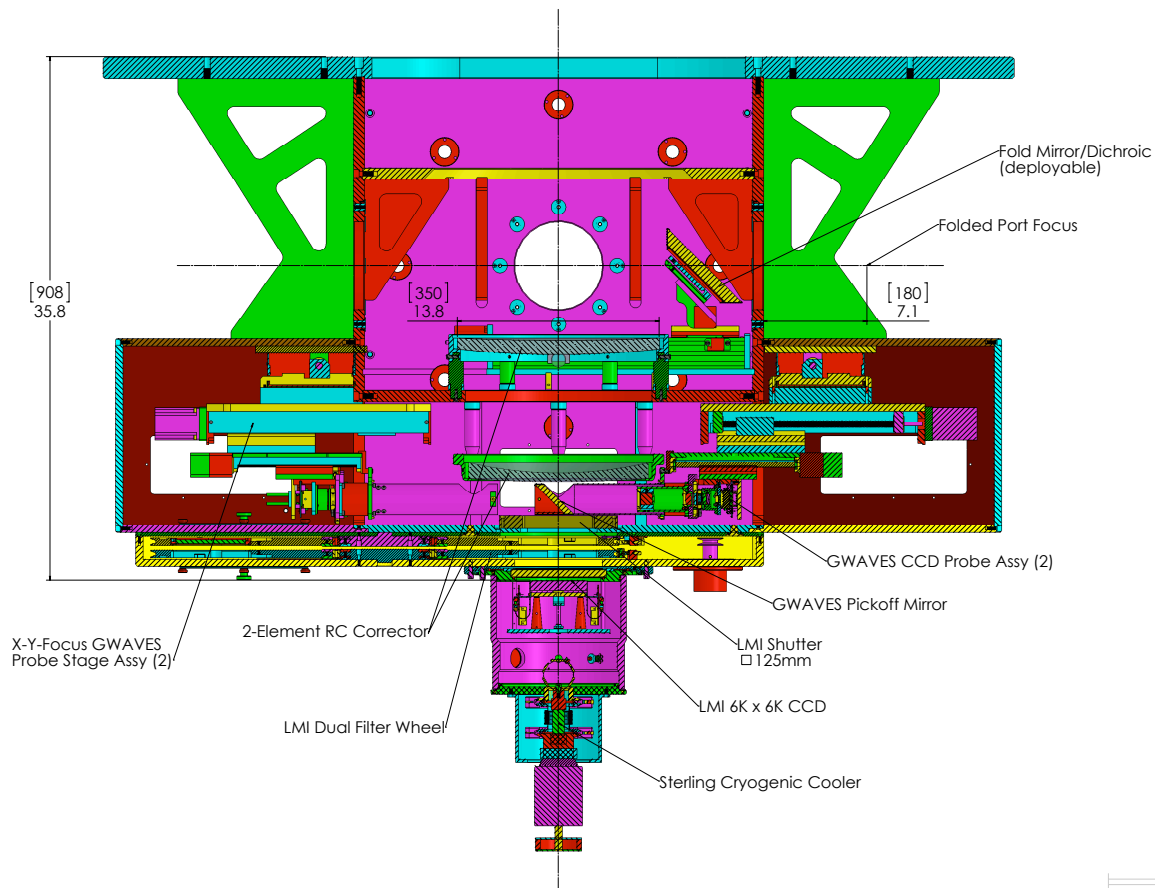

Figure 4. Cross sectional model view of the RC instrument cube assembly, including the RC corrector lenses, GWAVES probe assemblies, and the LMI filter wheel and camera assemblies.

The assembly includes mechanical interfaces for 4 additional instruments to be mounted on the cube's sides, to utilize focal planes located 180mm behind the mounting surfaces. Two of the instrument ports are appropriate for smaller instruments up to about 65kg mass, being located just above the cube enclosures containing the GWAVES 3-axis probe assemblies, as shown in Figure 4. The other 2 ports will support larger instruments up to 360kg (the faces in-plane with Figure 4), providing a much larger volume available for longer focal length instruments or those with more complicated geometries. Figure 5 shows a rendering of the instrument cube with 3 first-light instruments and GWAVES and LMI support electronics assemblies installed. The early operations instrument complement is described in further detail in the DCT status paper[1].
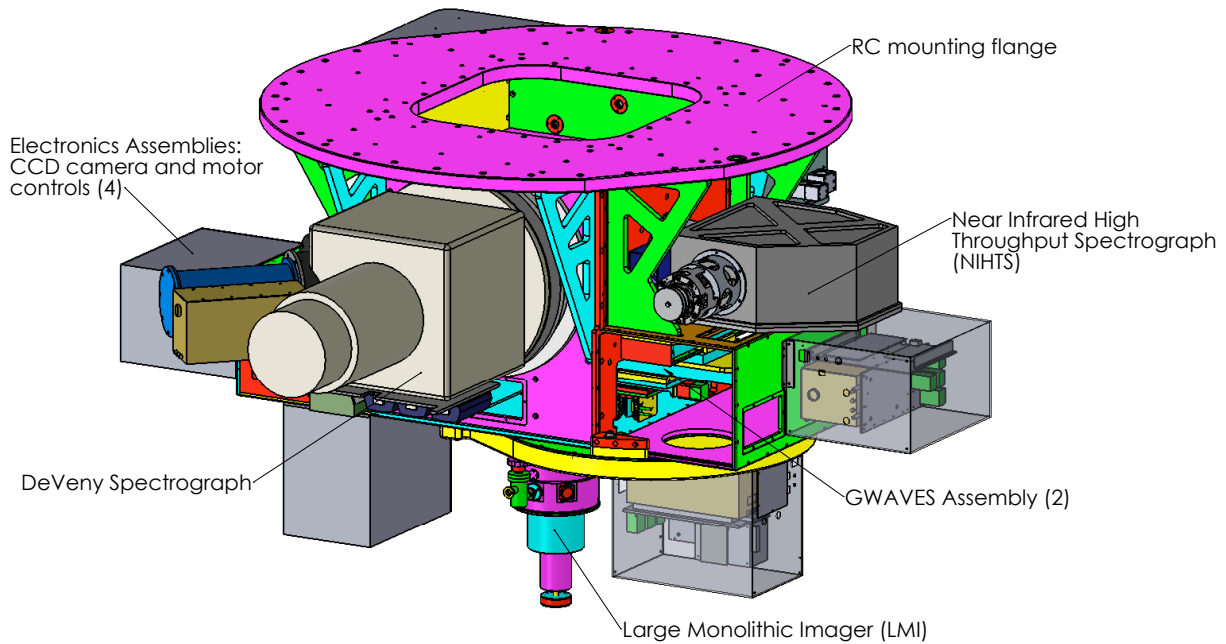

Figure 5. Model of the instrument cube with 3 first-light instruments installed: the LMI with dual filter wheel at the straight-through port, the DeVeny Spectrograph at a large instrument port, and the Near Infrared High Throughput Spectrograph (NIHTS) at a small instrument port.

The instrument cube structure must be stiff enough to prevent excessive flexure between the instrument focal planes and the guider probes as gravitational loading changes with telescope tracking. The assembly orientation varies from zenith to horizon pointing, and 540° total travel of the Cassegrain instrument rotator. During a long scientific instrument exposure, image degradation from instrument-guider flexure should be less than that introduced from jitter in telescope tracking. We therefore conducted a finite element analysis (FEA) of the cube structure model to determine its structural rigidity and indicate where additional stiffening support was needed[6]. The cube was modeled as a fused 6061-T6 Al structure within the SolidWorks simulation package, with masses attached representing instruments, guider assemblies, and the RC corrector assembly. The deflections of nodes at the location of the guider probe foci relative to the 5 instrument foci were calculated for the zenith and 2 horizon pointing orientations, to determine the magnitudes of translation (guider error) and piston (focus error). The guiding and focus errors were compared to DCT requirements for closed-loop tracking jitter (0.083 arcsec FWHM) and closed-loop M1-M2 relative position (0.0018 arcsec FWHM), for maximum deflection over a 15° (1 hr) position change on the sky.

The cube model was initially constructed with a 1" main flange and simple box enclosures with no internal support, intended to be as lightweight as possible. The resulting deflections yielded a guide error of 1 arcsec hr^{-1}, approximately 12 times the jitter goal. Two internal bulkheads were added for the 2nd iteration, with only a small improvement to 0.75 arcsec hr^{-1} guide error. The dominant contribution to guide and focus errors in these models was the flexibility of the 1" mounting flange, with a deflection of 0.3mm at the center of the flange relative to the bolt circle at the edge. We therefore thickened the flange to 1.5", and added 8 external gusset supports to bridge a partial load to the attachment bolt

circle. In addition to the internal bulkheads, a network of internal trusses were also added to preserve the squareness of the structure. A rendering of the final magnified FEA deflections for the zenith loading case are shown in Figure 6, where the flange center deflection was reduced to approximately 8μm. The final model maximum guide error is 0.05 arcsec hr^{-1} for a 360kg instrument mass attached to a large instrument port.
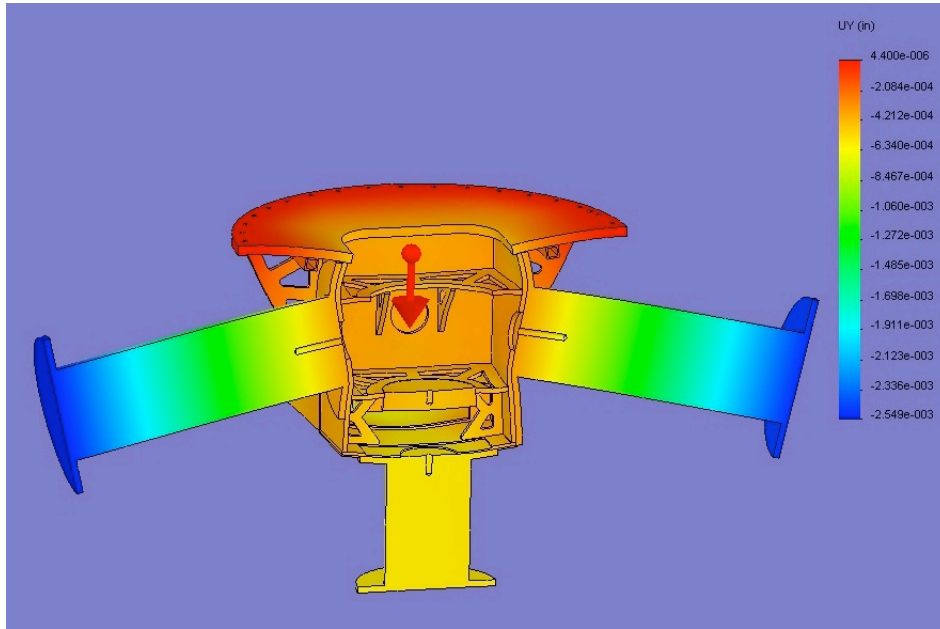

Figure 6. Finite element analysis simulation of an overloaded cube model (362kg instrument masses). The deflection of the center of the mounting flange relative to the bolt circle at the edge is approximately 8μm.

The linear stages supporting the GWAVES probes will also deflect according to the stiffness of the stages and the camera assembly. The commercial stages selected are fine pitch, lead screw driven with a specified stiffness of 0.026 arcsec in^{-1} lb^{-1} in pitch or roll. The loads on the stages are approximately 37lb for the X-stages, and 17lb for the Y-stages, applied over a lever arm of approximately 17.7". The resulting stage flexure for full deflection would be 0.054 arcsec and 0.025 arcsec for the X and Y stages, respectively, with a maximum 15° (1 hr) deflection of 0.008 arcsec. We therefore estimate the maximum guide error to be 0.058 arcsec hr^{-1} for the cube and GWAVES assemblies, less than the DCT jitter specification of 0.083 arcsec RMS.

4. RC CORRECTOR OPTICS

The DCT RC optical design, coupled with the telescope's mechanical layout and baffling, delivers a 0.5° unvignetted FOV to the RC focal plane. Over small field angles, up to approximately 5 arcmin FOV, the image degradation due to RC off-axis astigmatism and field curvature (defocus) is small compared to expected instrumental contributions, on the order of 5μm RMS spot broadening or 0.06 arcsec FWHM. Therefore, it is not necessary to correct the beam delivered to the folded instrument ports on the cube. However, the field curvature of the 0.5° focal surface is approximately 3mm, with off-axis astigmatism of 2 waves (at 0.5 microns/wave) at the 17.4 arcmin diameter corners of the e2v 6K x 6K CCD. Left uncorrected, the resulting image quality at the corners of the LMI field would be 0.88 arcsec FWHM. For imaging instruments such as the LMI, and future instruments that will exploit the entire 0.5° DCT FOV, it is therefore necessary to flatten and correct the focal plane to preserve the wider field image quality.

A major scientific driver for the LMI is the need to do surface photometry to very faint levels, i.e. m(B,V) ~ 30 mag arcsec^{-2}, in order to study the outer reaches of galaxies. Internal reflections within the LMI beam path produce ghost images on the CCD, which are introduced both from stars within the field and the uniform sky background. The

brightness of ghost images depends critically on the shape and location of the optical surfaces, as well as the anti-reflection (AR) coatings applied to the optics. Ghost pupil images can be particularly troublesome[7] and have been avoided in the optical design. Other important requirements for the system are high UV transmission and low distortion.

Design of an optimized RC corrector is a straightforward exercise[8]; a conceptual corrector for the DCT was presented several years ago[9]. However, the very low ghost surface brightness requirement and the need to package the corrector in the cube with the guider and retractable fold mirrors for the other instruments significantly complicated the design. In addition we require the ability to add a removable atmospheric dispersion corrector (ADC) at a future date without compromising the performance.

We have developed a 2-element fused silica corrector that meets the stringent requirements of the LMI and instrument cube assembly. The lens mountings are shown in Figure 1, located between the folded ports axis and the GWAVES camera probes. The lenses are mounted athermally for zero-stress with temperature changes, by use of zinc-plated ASTM-36 steel cells with an elastomer providing the bond between glass and cell. The elastomer chosen is Sylgard 184, with bead thicknesses of approximately 7mm, that correspond to its coefficient of thermal expansion of 2.7×10^{-4} C^{-1}.

The DCT error budget allocated 0.085 arcsec FWHM (6.6μm RMS) image degradation due to the corrector optics for the delivered 0.5° FOV. Within the FOV of the LMI (0.205° square), the corrector design delivers spot sizes from 4.2-6.4μm RMS over the wide bandpass covering B through I-bands (360-860nm). At a field diameter of 0.5°, the spot size is 5.3μm RMS for the VR band, where 7.5μm encloses 80% of the encircled energy. The LMI differential distortion goal is 1% over its FOV, and the design produces 0.03% distortion.

Ghost images were examined using the ghost focus generator in Zemax. Internal reflections occur between all surfaces of the LMI optical train including a future atmospheric dispersion compensator located forward of the instrument cube. Ghost image sizes were calculated based on the marginal ray height at the CCD, and the fractional sky illumination increase due to these reflections were computed for reflective surfaces of 1-2%. Assuming 1% AR coated surfaces, the total increase in sky illumination due to reflections internal to the RC corrector was 0.025%, and that due to reflections from all other surfaces and the corrector totaled 0.059%. The brightest ghost internal to the corrector for an M8 star would be 26.75 mag arcsec^{-2}, approximately 8mm in diameter and converging; this type of ghost would not increase the wider field sky background, however. The brightest stellar reflection that would degrade surface photometry occurs in a diverging reflection between the surfaces of element 1; the luminance from this ghost for an M8 star would be 30.2 mag arcsec^{-2}, meeting the LMI requirement for ghost pupil images. Two other reflections between filter and corrector surfaces are of similar magnitude for 1% surfaces but the actual filter coatings may be more reflective than this. All other LMI system internal reflections are fainter than the specification.

The multi-layer AR coatings for the 4 corrector and 4 dewar window (including a spare window) surfaces were applied by Infinite Optics, with the reflectance results shown in Figure 7 with the LMI filter transmission band edges. The largest average reflectance from witness samples over 300-650nm is 0.78%, and that over 650-1100nm is 0.89%; transmission is 98.5% and 98.6% over these bandpasses, respectively. As the average reflectances are less than 1% overall, the luminance of ghost reflections described above should be upper limits in practice. The coatings are hard and can be cleaned with standard solvents.
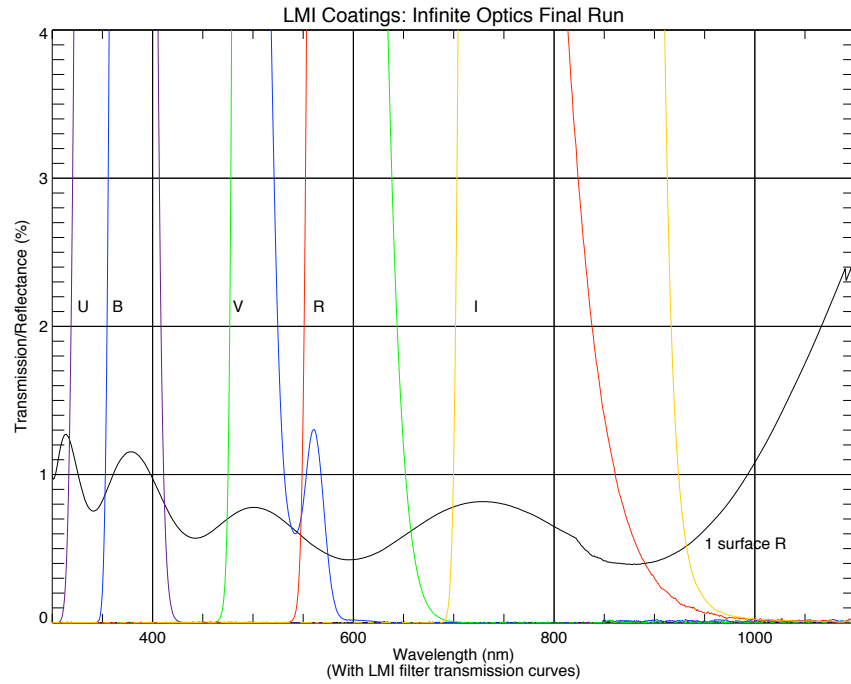
Figure 7. Reflectance of the AR coatings applied to the RC corrector lenses and LMI dewar window surfaces, plotted with the LMI filter transmission curves. The labels UBVRI indicate the rising edges of the filter transmission curves, with the falling edges in the same color plotted redwards of each in turn.
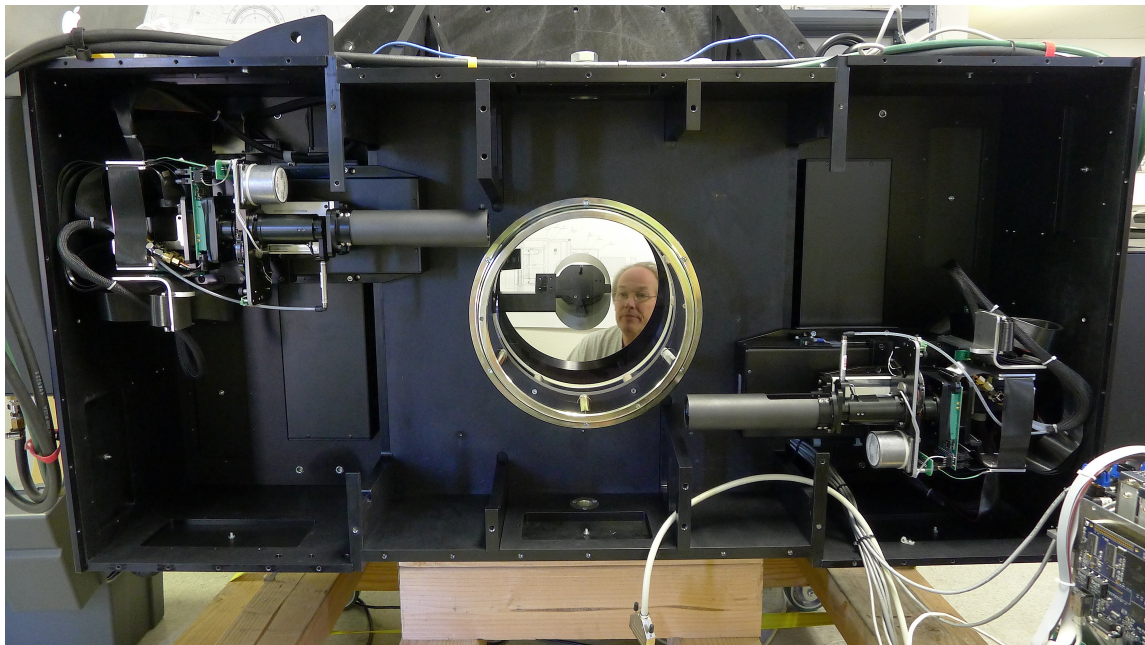

Figure 8. The RC instrument cube with the back plates removed, showing the GWAVES probe assemblies and translation stages, and looking through the RC corrector lenses to a fold mirror deployed into the center of the cube.

5. GWAVES CCD Camera Probes

At the core of the instrument cube are the two GWAVES probes, each of which serves dual functions as either a guider or wavefront sensor. Each probe acquires guide or WFS stars in the RC FOV by 2-axis motion in the corrected beam, injecting a field star into reimaging optics system with a 50mm diameter pickoff mirror. An early study of available commercial CCD cameras revealed that our tight space requirements and the need for operational flexibility and compatibility with existing instrument software could only be satisfied with cameras built in-house. The CCD cameras utilize e2v CCD67 frame transfer devices with 256 x 256 26μm pixels (0.36 arcsec/pixel), mounted in an e2v thermoelectric cooler package with facility glycol plumbed through the head. The cameras are driven with Leach Gen-III CCD controllers, operated with Linux server workstations running the Lowell Observatory Instrumentation System (LOIS)[10].   As part of the GWAVES project, LOIS was migrated to the Linux-based operating system from the Sun/Solaris platform, for easier future portability of all Lowell-built cameras and use of the PCI-X Leach fiber interface. Operation of the CCD cameras on the movable probes required the addition of preamplifiers at the CCD socket board to drive the signals over approximately 2m of ribbon cable to the controllers mounted on the enclosure. The GWAVES software will be described in a future technical report.

The as-built GWAVES probe is shown in Figures 9 and 10. The assembly includes the diagonal pickoff mirror mounted in a thin and stiff steel tube which is attached to the Y-axis of the moving probe stages. The camera reimaging optics are mounted within a camera assembly that includes a comparison LED and pinhole with beamsplitter, an air-actuated stop to reduce sky background for wavefront sensing, an 8-position filter wheel with home and detent mechanical switches and 2 MLM-position magnetic reed switches, and the CCD head assembly. The camera assembly is mounted on a focus stage with 100mm of travel to accommodate changes in telescope focus position with temperature. To allow for 3-axis motion with up to 300mm travel in the probe positions, four ribbon cables to drive the CCD and filter wheel, 2 glycol lines, and an air line are routed through strain relief brackets with service loops which unwind as the assembly moves.
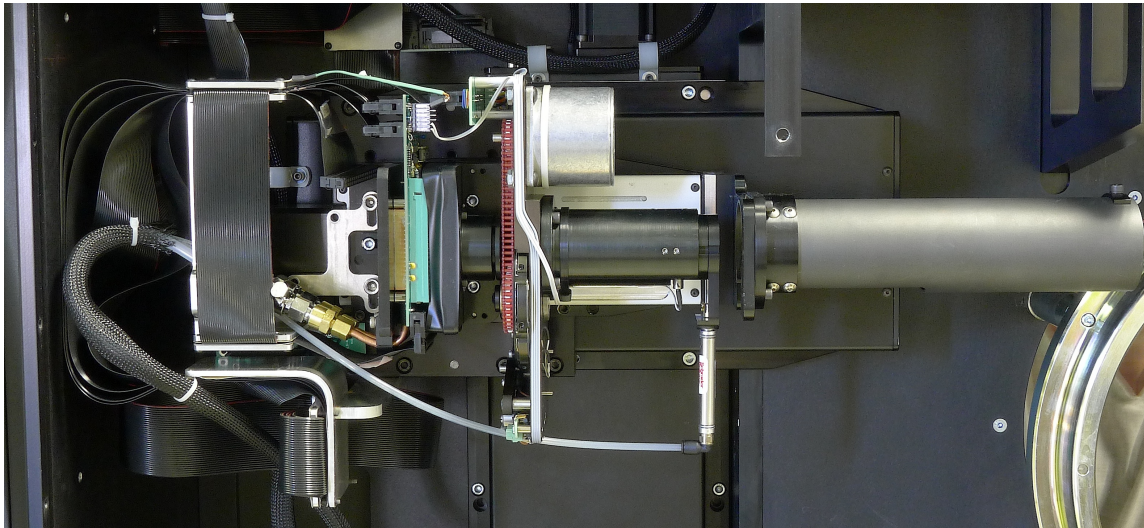

Figure 9. A GWAVES probe pictured from behind. The CCD chips are mounted in an e2v thermoelectric cooler package, and the heads are cooled with facility glycol. The WFS sky suppressor stop is actuated with a small air solenoid.
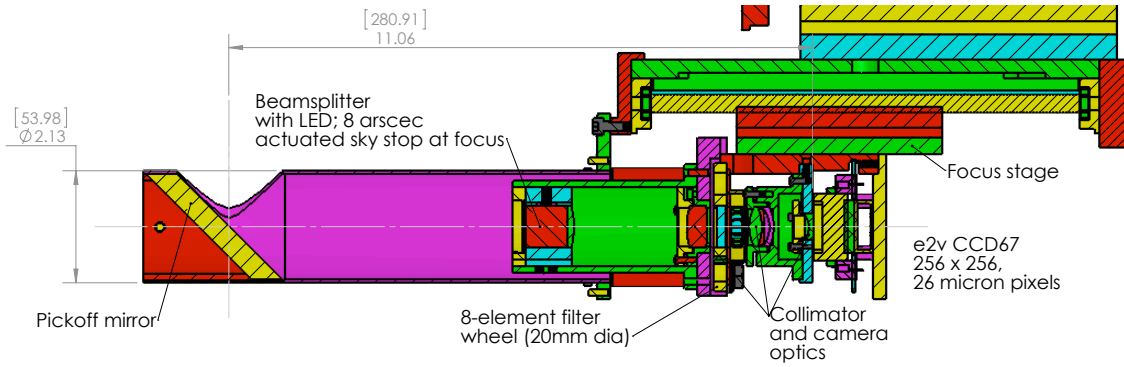
Figure 10. A GWAVES probe model shown in cross section. The entire camera assembly including the beamsplitter/LED mount is focused independently behind the pickoff mirror which is attached separately to the X/Y stages above.

The probe reimaging optics reduce the f/6.1 DCT RC focal ratio to f/3.9, increasing the FOV available imaged on the CCD to 92 arcsec[2]; the optical prescription is shown in Table 3. The custom lenses were fabricated by Optimax, Inc, and there are 2 stock lenses included. The collimator lenses are greased together for optical contact, as is the field flattener to the CCD window. The design features both a direct imaging system for guiding, and an afocal Shack-Hartmann configuration by a simple change of filter at the internal pupil[11]. The 8-element filter wheel carries a Bessel UBVR filter set, and 2 multi-lenselet modules (MLM) bonded to negative lenses to support coarse and fine wavefront sampling, detailed in Table 4. A custom beamsplitter located behind the telescope focus serves to direct the light from an LED into the system for wavefront calibration. The beamsplitters were assembled from stock prisms that received a 1% AR coating on the LED reflecting faces, and bonded together with the plano-convex field lens located on the back surface.

Table 3. Optical prescription of the DCT, RC corrector, and GWAVES probe (WFS mode)				
Element	Radius (mm) (Conic constant)	Thickness and/or Separation (mm)	Material	Diameter (mm)
Primary mirror	-15994.42 (k1=-1.0828)	5619.70	ULE	4280
Secondary mirror	6925.79 (k2=-4.5029)	7212.24	Fused silica	1360
RC corrector Element 1	-3658.61 (front) -1509.66 (back)	25.0 204.8	Fused silica	350
RC corrector Element 2	-699.84 (front) -2007.46 (back)	15.0 30.24	Fused silica	310
Pickoff mirror	Infinite	135.39	Pyrex	70
Beamsplitter	Infinite	20.0	BK7	20
Field lens	Infinite (front) -36.33 (back)	3.4 54.22	BK7	20
Collimator lens 1	34.96 (front)	2.01	KZFS11	20
Collimator lens 2	12.0 (front) -82.62 (back)	8.0 4.64	FK51A	20
0768-86 MLM	39.6 (lenslet) 46.71 (back)	12.52	BK7	9.92
Camera lens 1	20.38 (front) -23.05 (back)	6.11 3.72	FK51A	19
Camera lens 2	-15.175 (front) -23.224 (back)	2.03 16.94	KZFS11	19
Field flattener	-10.38 (front)	2	BK7	12.7
CCD window	Infinite	2.5	BK7	12.7
CCD67				9.4

Table 4. Wavefront Sensing Optical Specifications				
Lenselet Array (pitch/focal length (mm)	Effective focal length (mm)	Spot separation (mm/pixels)	M1 subaperture diameter (mm)	Capture range (arcsec)
1.750 / 90	14470	0.73 / 28	790	5.2
0.768 / 86	14110	0.33 / 12.7	330	2.1

The GWAVES probes were assembled and tested in the laboratory in both direct imaging and WFS modes, located behind a custom f/6.1 artificial star projection system. The test image quality with no filter was 22μm RMS and 20μm with a V-band filter; the latter spot size would degrade the site median image quality by approximately 12%. The WFS tests involved analysis of spot patterns imaged with the coarse and fine MLM filter wheel positions, with no equivalent secondary obscuration. The imaged spot patterns compared well to Zemax simulations of the patterns for aperture sampling and spot separations. Aberrations were introduced into the artificial star by defocusing of the probe assembly and rotation of the collimating lens in the artificial star system to induce astigmatism and coma. The GWAVES Shack-Hartmann analysis package (S.6 below) was used to measure the wavefronts, and the results showed agreement between the Zemax simulations and the measured wavefront of less than 0.05 wave for the introduced focus, X-astigmatism, and Y-coma Zernike terms (Z_4, Z_6, and Z_7), with the magnitude of all other terms up to $Z_{11} < 0.02$ wave.

6. DCT TEST INSTRUMENTATION AND
GWAVES INSTALLATION AND TESTING

The path to construction of GWAVES and the instrument cube included the development of two DCT test instruments: the Pointing Telescope, and the Prime Focus Test Assembly (PFTA). The pointing telescope consisted of a 6" f/15 objective lens previously used in the guide telescope of the Perkins Schmidt camera, a folding flat, and a 50mm FL Barlow lens imaging onto an e2v 512 x 512 CCD57 frame transfer CCD with 13 micron pixels. The CCD camera project included the first adaptation of the LOIS control software to a Linux-based host computer operating a Leach Gen-III CCD controller with a PCI-X interface. The pointing telescope was installed on the DCT mount following its assembly at Happy Jack in Sept. 2010, in order to prove the telescope's pointing and tracking abilities prior to installation of the telescope's primary mirror. The first pointing maps for the telescope were created with the use of this system, and the final map was subsequently used as the baseline map following installation of M1. Also, rudimentary guiding was conducted which helped to refine the TCS guider gain and compensator parameters to stable values, and resolve some ambiguities in the algorithms.

The PFTA was developed in order to conduct on-sky tests of the M1 AOS in the 6-month interval between the installations of M1 and M2. It consisted of a f/1.7 90mm dia 2-element M1 corrector with a 0.2° FOV, a 6-element f/6.1 reimaging system, and a complete GWAVES probe assembly without pickoff mirror (Figure 11). The optics and camera system were mounted on a bench assembly and attached to the M2 support cage on the top end by means of a welded stool structure. As prime focus and the PFTA are located behind the cage, there was asymmetric vignetting of the beam by the cage structure, affecting the accuracy of the wavefront slope solutions but not preventing the goals of the tests to be met. Initially, there was approximately 7mm of decenter of the PFTA to the M1 beam, detected with the WFS camera as coma, and corrected by adjustment of push screws on the optics and camera enclosure. Once aligned, the system was used on sky over approximately 16 weeks to test and refine the Zernike polynomial to bending mode wavefront representation, the application of bending modes to M1, the elevation dependence of M1/M2 collimation and focus, and to serve as a development platform for the GWAVES and WFS software suite. The tests importantly demonstrated that neither the mounting and active support of M1, or the optical support structure for the top end, exhibited hysteresis in the wavefront when the telescope was repeatedly scanned in elevation from near zenith pointing to low elevation.
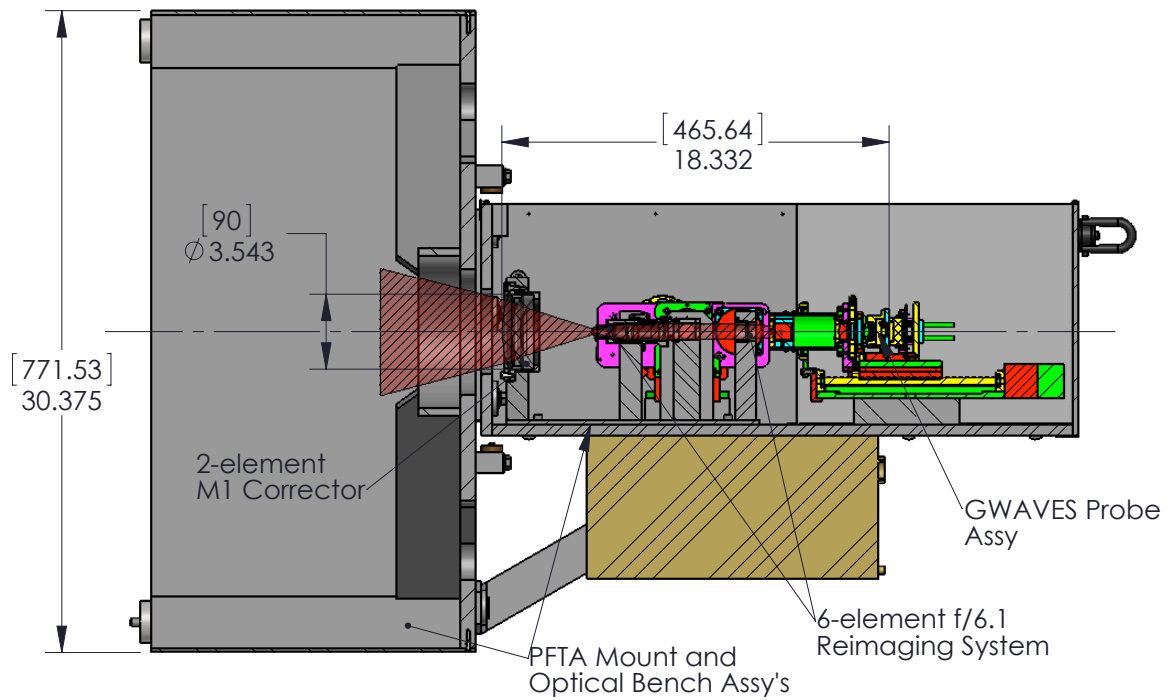
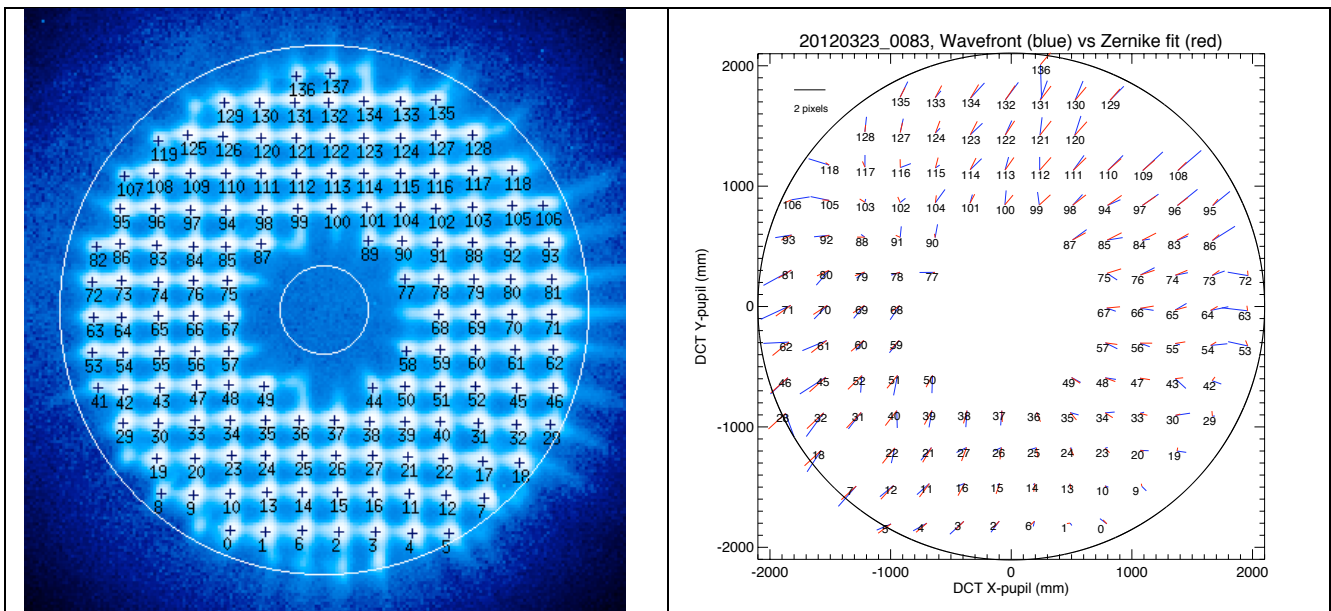Figure 11. Cross sectional view of the Prime Focus Test Assembly (PFTA) model.

Figure 12. Shack-Hartmann image taken on-sky with the 0.768-86mm fine MLM (left), and an analysis plot showing measured and fit vector slope displacements.

The RC instrument cube assembly was integrated in Dec. 2011 and Jan. 2012 in Lowell's Mars Hill instrument laboratory, and installed on the DCT Cassegrain rotator in early Feb. 2012 following the installation of M2 on the telescope. On-sky testing at the RC focus began soon thereafter, beginning with pointing and probe position calibrations, and WFS verification tests with the associated coordinate transformations. The GWAVES-sampled DCT wavefront has been analyzed in near-real-time (closing the M1/M2 correction loop manually) and with batch post-processing. The imaged MLM spot patterns are processed to derive the wavefront expressed as an expansion in Zernike coefficients[12] by means of a custom IDL-based package that solves a nonlinear least-squares fit to the wavefront slope. Examples of a WFS stellar image and wavefront solution are shown in Figure 12. Early optical testing of the fully assembled DCT concentrated on so-called elevation scans, taking WFS samples without sending corrections, on stars from elevations of 85° to 10° in 15° increments and back again. These scans have demonstrated that decenter and piston deflections of the M2 top end follow expected dependencies on the change in load vector, namely deflecting in piston as cos(zenith angle (ZA)), and in decenter as sin(ZA). The zenith angle dependence of focus is shown in Figure 13, where Z_4 solutions are plotted for several elevation scans taken in March 2012 along with the cos(ZA) fit. When the fitted function is subtracted from the data, and the residuals are plotted vs. the mount temperature as shown in Figure 14, a linear relationship of Z_4 vs. temperature emerges. While the temperature range of 2° C represented is narrow, extending these tests into summer temperatures will serve to verify the relationship. The ultimate objective of such elevation scans is to formulate lookup tables for the complete set of M1 bending mode and M2 piston and tip-tilt corrections that will be applied in open-loop control of the DCT AOS during regular operations[13].

On-sky testing of the DCT with GWAVES will continue in the 2nd half of 2012 in preparation for the initial science operations planned to begin in 2013. The LMI camera will be installed in this period as well, providing a very important and unique facility science instrument to incorporate software tools for scientific work and demonstrate the full system capabilities.
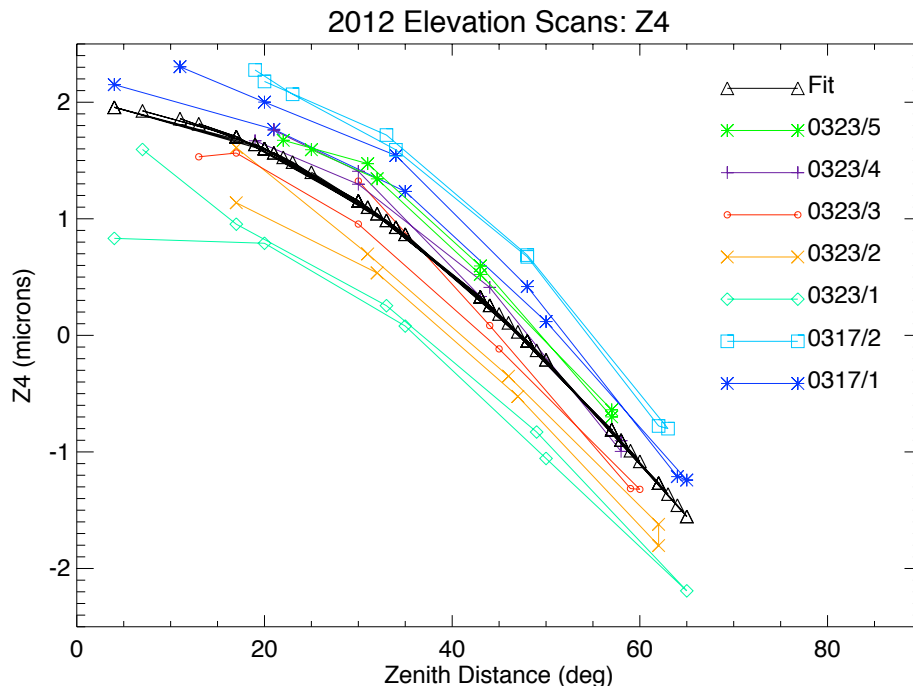

Figure 13. Shack-Hartmann wavefront sensor measurements of Zernike polynomial 4 (focus), as the DCT is stepped down in elevation from the zenith to 25° elevation and back. The data has been fit with a cosine function vs. zenith distance (angle).
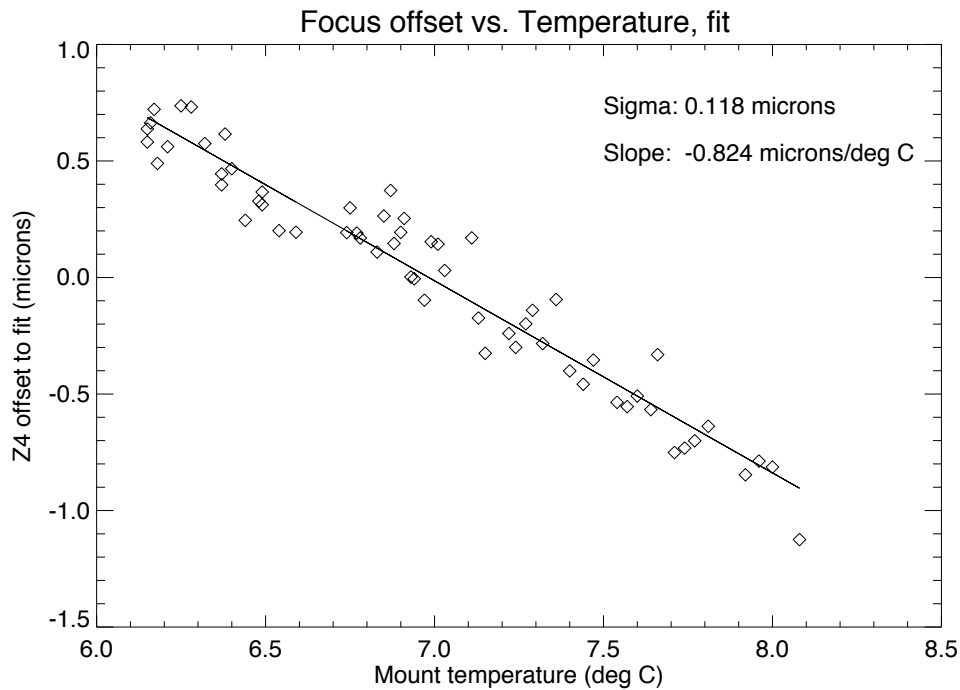
Figure 14. The focus residuals from Figure 12 after subtraction of the fitted despace of M2, then fit with a linear solution for temperature dependence of focus.

ACKNOWLEDGMENTS

REFERENCES

[1] Levine, S. E., Bida, T. A., Chylek, T., Collins, P. L., DeGroff, W. T., Dunham, E. W., Lotz, P. J., Venetiou, A. J., and Zoonemat Kermani, S., "Status and performance of the Discovery Channel Telescope during commissioning", Proc. SPIE 8444-44 (2012).

[2] Bida, T. A., Dunham, E. W., Bright, L. P., and Corson, C., "Site testing for the Discovery Channel Telescope", Proc. SPIE 5489, 196-206 (2004).

[3] Massey, P. L., Dunham, E. W., Bida, T. A., Hunter, D. A., and Schleicher, D. G., "A large monolithic imager for the Lowell Observatory 4.2-meter Discovery Channel Telescope",   http://www.lowell.edu/dct_instruments_lmi.php#, (2012).

[4] Dunham, E. W., and Eliot, J. L., "Limiting magnitudes for SOFIA IMC camera systems", SOFIA TN-EWD-001.R1 (1998).

[5] Bida, T. A., "GWAVES functional, performance, and control software requirements", DCT-0500--004-A (2010).

[6] Chylek, T., "RC Guider and Wavefront Sensor FEA design report", DCT-0560A-041, 042, 043-A (2011).

[7] Jacoby, G. H., Liang, M., Vaughnn, D., Reed, R., and T. Armandroff, "A new wide-field corrector for the Kitt Peak Mayall 4-m telescope", Proc. SPIE 3355, 721-734 (1998).

[8] Epps, H. W. and Fabricant, D., "Field correctors for wide-field CCD imaging with Ritchey-Chretien telescopes", AJ 113, 439-445 (1997).

[9] MacFarlane, M. J. and Dunham, E. W., "Optical design of the Discovery Channel Telescope", Proc. SPIE 5489, 796-804 (2004).

[10] Taylor, B. W., Dunham, E. W., and Elliot, J. L., "Performance of the Lowell Observatory Instrumentation System", Proc. SPIE 5496, 446-454 (2004).

[11] Pernechelle, C., Bortoletto, C.F., Fantinel, D., and Giro, E., "Afocal Shack-Hartmann screen for an instrument with an accessible pupil", PASP 112, 996-1000 (2000).

[12] Noll, R.L., "Zernike polynomials and atmospheric turbulence", JOSA 66, 207-211 (1976).

[13] Venetiou, A. J., and Bida, T. A., "Discovery Channel Telescope active optics early integration and test", Proc. SPIE 8444-49 (2012).